

Analysis of Coding RNA and LncRNA Expression Profile of Stem Cells from the Apical Papilla After Depletion of Sirtuin 7

Lu Yuan JIN^{1,2}, Lei HU^{1,3}, Hui Na LIU¹, Deng Sheng XIA², Zhi Peng FAN¹

Objective: To explore the effects of Sirtuin 7 (SIRT7) on the gene expression profile of stem cells from the apical papilla (SCAPs).

Methods: SCAPs were isolated and cultured. SIRT7 short hairpin ribonucleic acid (shRNA) was used to knock down the expression of SIRT7 in SCAPs. After library construction and RNA sequencing (RNA-seq), differentially expressed genes were identified using Cuffdiff with a false discovery rate (FDR) ≤ 0.05 and fold change ≥ 2 . Pathway and Gene Ontology (GO) analyses were conducted to elucidate the changes in important functions and pathways after SIRT7 gene knockdown. Gene set enrichment analysis (GSEA) was performed and enrichment of a gene set with an FDR lower than 0.25 was considered significant.

Results: The most striking GO terms related to SIRT7sh SCAPs and Consh SCAPs were response to nucleus, nucleolus, cytoplasm, protein binding and intrinsic apoptotic signalling pathway. Signalling pathway analysis revealed the top five pathways to be metabolic, pyrimidine metabolism, protein processing in endoplasmic reticulum, phosphatidylinositol 3-kinase/protein kinase B (PI3K/Akt) signalling and p53 signalling. The results of GSEA showed that genes were mainly enriched in cell cycle, cell proliferation, transforming growth factor beta (TGF- β) signalling and cytokine–cytokine receptor interaction pathways.

Conclusion: SIRT7 may affect the functions of SCAPs through cell cycle, cell proliferation and apoptosis pathways.

Key words: RNA sequencing, SIRT7, stem cells from the apical papilla
Chin J Dent Res 2020;23(3):169–176; doi: 10.3290/j.cjdr.a45220

1 Laboratory of Molecular Signalling and Stem Cells Therapy, Beijing Key Laboratory of Tooth Regeneration and Function Reconstruction, Capital Medical University School of Stomatology, Beijing, P.R. China.

2 Department of General Dentistry and Integrated Emergency Dental Care, Beijing Stomatological Hospital, Capital Medical University, Beijing, P.R. China.

3 Molecular Laboratory for Gene Therapy and Tooth Regeneration, Beijing Key Laboratory of Tooth Regeneration and Function Reconstruction, Capital Medical University School of Stomatology, Beijing, P.R. China.

Corresponding author: Dr Zhi Peng FAN, Laboratory of Molecular Signalling and Stem Cells Therapy, Beijing Key Laboratory of Tooth Regeneration and Function Reconstruction, Capital Medical University School of Stomatology, No. 4 Tiantanxili, Dongcheng District, Beijing 100050, P.R. China. Tel: 86-10-57099311; Fax: 86-10-57099311. Email: zpfan@ccmu.edu.cn

This work was supported by grants from the Young Elite Scientist Sponsorship Program by CAST (2016 QNRC001 to LYJ).

Stem cells from the apical papilla (SCAPs) are mesenchymal stem cells isolated from the apical papilla of immature permanent teeth¹. They are multipotent stem cells that possess high proliferative potential, the capacity for self-renewal and low immunogenicity². Moreover, they can differentiate into many cell types, such as osteocytes, chondrocytes and nerve cells. Therefore, SCAPs have been widely studied in tissue engineering and regenerative medicine³. However, some problems still limit their clinical application, for example if the source of seed cells is limited and mechanisms of directional differentiation are unknown. It is therefore important to elucidate the mechanism that affects the function of SCAPs.

The sirtuin family comprises seven members that play significant roles in regulating various important biological processes including ageing, transcription, DNA repair, genomic stability, apoptosis, inflammation

and stress resistance^{4,5}. Sirtuin 7 (SIRT7) is a member of this family and influences various biological processes including the cell cycle, stress resistance, ageing and tumorigenesis⁶⁻⁸.

SIRT7 affects stem cell proliferation. A study revealed that in aged human stem cells (HSCs), SIRT7 had a lower expression level, which led to increased apoptosis and decreased proliferation rate. When SIRT7 was reimported into aged HSCs, their regenerative capacity was partially restored⁹. A recent study¹⁰ provided further important clues regarding the role of SIRT7 in dental pulp stem cell (DPSC) senescence. SIRT7 was a direct target gene of microRNA-152 (miR-152), both of which regulated the senescence of DPSCs. Overexpression of miR-152 induced senescence and inhibited proliferation of DPSCs concomitant with downregulation of SIRT7. Overexpression of SIRT7 almost prevented miR-152-induced senescence entirely. It was also reported that SIRT7 played a role in the differentiation of mesenchymal stem cells. SIRT7 knockdown in human bone marrow stem cells (hBMSCs) significantly enhanced osteoblast-specific gene expression, alkaline phosphatase activity and mineral deposition *in vitro*, which was partially regulated by the wingless-related integration site/ β -catenin (Wnt/ β -catenin) pathway¹¹. However, during the osteogenic differentiation of DPSCs, no significant change was found in SIRT7¹².

The function and mechanism of SIRT7 in SCAPs have not been previously explored. In this study, RNA sequencing (RNA-seq) between SIRT7sh SCAPs and Consh SCAPs was used to detect the possible function and mechanisms of SIRT7 in SCAPs.

Materials and methods

Cell cultures

Dental tissues were obtained under approved guidelines set by Beijing Stomatological Hospital, Capital Medical University (Ethical Committee Agreement by Beijing Stomatological Hospital Ethics Review No. 2011-02) with informed consent from the patients. Human wisdom teeth were first disinfected with 75% ethanol and then stored in phosphate-buffered saline (PBS) with 100 U/ml penicillin and 100 μ g/ml streptomycin (Invitrogen, Carlsbad, CA, USA) for no more than 4 hours. Subsequently, SCAPs were isolated and separated from the apical papilla of the root and then digested in a solution of 3 mg/ml collagenase type I (Worthington Biochemical, Lakewood, NJ, USA) and 4 mg/ml dispase (Roche

Diagnostics, Indianapolis, IN, USA) for 1 h at 37°C. Single-cell suspensions were obtained by passing the cells through a 70- μ m strainer (Falcon, BD Biosciences, Franklin Lakes, NJ, USA). SCAPs were grown in a humidified 5% CO₂ incubator at 37°C in Dulbecco's modified Eagle medium (DMEM) (Invitrogen) supplemented with 15% foetal bovine serum (Invitrogen), 2 mmol/l glutamine, 100 U/ml penicillin and 100 mg/ml streptomycin (Invitrogen). The culture medium was changed every 3 days. Cells passaged to the fourth and fifth generation were used in further experiments.

Plasmid construction and viral infection

Plasmids were constructed using standard methods, and all structures were verified by appropriate restriction digestion and/or sequencing. Short hairpin ribonucleic acids (shRNAs) with complementary sequences of SIRT7 were subcloned into the lentiviral vector pLKO.1 (GenePharma, Suzhou, China). Viral packaging was prepared according to the manufacturer's protocol (GenePharma). For viral infections, SCAPs were plated overnight and then infected with lentiviruses in the presence of polybrene (6 mg/ml, Sigma-Aldrich, St. Louis, MO, USA) for 12 h. After 48 h, infected cells were selected with 2 mg/ml puromycin for 7 days. LV3 shRNA (Consh, control shRNA) was purchased from GenePharma as a control. The target sequences for the shRNA were SIRT7 shRNA (SIRT7sh): 5'-GGAAGTGTGATGACGTCATGC-3' and LV3 shRNA (Consh): 5'-GTGCGTTGCTAGTACCAAC-3'.

Library construction for RNA-seq and sequencing procedures

SCAPs were seeded in 10 cm² dishes and cultured until 80% confluence was reached. Total RNA was isolated from SCAPs using the RNeasy Mini Kit (Qiagen, Hilden, Germany). Paired-end libraries were synthesised using the TruSeq RNA Sample Preparation Kit (Illumina, San Diego, CA, USA) following the TruSeq RNA Sample Preparation Guide. The polyadenylate (poly[A])-containing mRNA molecules were briefly purified using poly-T oligo-attached magnetic beads (Thermo Fisher Scientific, Waltham, MA, USA). Purified libraries were quantified with the Qubit 2.0 Fluorometer (Life Technologies, Carlsbad, CA, USA) and validated with the Agilent 2100 Bioanalyzer (Agilent Technologies, Santa Clara, CA, USA) to confirm the insert size and calculate the molar concentration. A cluster was generated using cBot (Illumina) with the library diluted to 10 pm and then sequenced on the HiSeq X Ten (Illumina). The

library construction and sequencing were conducted at Shanghai Biotechnology Corporation.

Data analysis

Sequencing raw reads were preprocessed by filtering out ribosomal RNA (rRNA) reads, sequencing adapters, short fragment reads and other low-quality reads. TopHat v2.0.9¹³ was used to map the cleaned reads to the mouse mm10 reference genome with two mismatches. After genome mapping, Cufflinks v2.1.1¹⁴ was run with a reference annotation to generate fragments per kilobase of exon model per million reads mapped (FPKM) values for known gene models. Differentially expressed genes were identified using Cuffdiff¹³. The *P* value significance threshold in multiple tests was set by FDR. The fold changes were also estimated according to the FPKM value in each sample. The differentially expressed genes were selected using the filter criteria of $FDR \leq 0.05$ and fold change ≥ 2 .

Gene Ontology (GO) analysis

To explore the biological function of the different genes involved, Gene Ontology (GO, <http://www.geneontology.org>) terms and the Kyoto Encyclopaedia of Genes and Genomes (KEGG, <http://www.genome.jp/kegg/>) pathway enrichment analysis were conducted using the clusterProfiler^{15,16}. Fisher exact test and *P* values were used for the detection and selection criteria. Significant GO terms or pathways were differentially expressed as gene > 2 and *P* value < 0.05 .

Long non-coding RNA (lncRNA) identification and expression analysis

Cufflinks was used to assemble reads into transcripts. Novel transcripts were obtained after comparing all the assembled transcript isoforms with the known mouse protein-coding transcripts using Cuffcompare¹⁴. Putative lncRNA were defined as novel transcripts set through the following filters: length ≥ 200 bp, number of exons ≥ 2 , open reading frame (ORF) ≤ 300 bp, no or weak protein-coding ability (Coding Potential Calculator [CPC] score < 0 ¹⁷ and Coding Non-Coding Index [CNCI] score < 0 ¹⁸ and no significant similarity with the Pfam database¹⁹). Finally, to generate a unique set of lncRNA, we used Cuffcompare to integrate the RNA-seq-derived lncRNA with the known lncRNA previously annotated with NONCODE v4. Differentially expressed lncRNA were selected for target prediction. The genes transcribed within a 10 kbp window upstream

or downstream of lncRNA were considered as cis-acting target genes. The trans-acting target genes were predicted using RNAplex software²⁰.

Gene set enrichment analysis (GSEA)

GSEA (www.broad.mit.edu/gsea) protocol was performed as described²¹. The association between phenotypes, biological processes/pathways and protein messenger RNA (mRNA) expression level was analysed. Predefined gene sets were obtained from the Molecular Signatures Database (MSigDB, <http://software.broad-institute.org/gsea/msigdb>): H, hallmark gene sets; CP, canonical pathways; and KEGG, KEGG gene sets). An FDR lower than 0.25 was considered to indicate significant enrichment of a gene set.

Statistical analysis

Each experiment was done independently and repeated at least three times with similar results. Results are expressed as mean \pm standard deviation (SD). Significant differences were assessed with a Student *t* test (two-tailed). $P < 0.05$ was considered statistically significant.

Results

Gene expression file by RNA-seq

SIRT7-shRNA constructs were transduced into SCAPs via lentiviral infection; ectopic SIRT7 expression was confirmed by real-time reverse transcription polymerase chain reaction (RT-PCR) analysis (Fig 1a) and western blot (Fig 1b). To investigate the possible function and mechanisms of SIRT7 on SCAPs, gene expression profiles of SIRT7sh SCAPs with Consh SCAPs were analysed using RNA-seq. When comparing SIRT7sh SCAPs with Consh SCAPs, there were 98 upregulated genes and 107 downregulated genes. The top 10 evidently changed genes are listed in Tables 1 and 2. Most of the genes with significant changes were correlated with cell apoptosis, cell cycle, cell proliferation and mitochondrial metabolism, including tyrosine 3-monooxygenase/tryptophan 5-monooxygenase activation protein gamma (YWHAG), heat shock protein family B (small) member 6 (HSPB6), tumour necrosis factor alpha-induced protein 1 (TNFAIP1), CDGSH iron sulphur domain 2 (CISD2), cyclin-dependent kinase 2-associated protein 1 (CDK2AP1), adenosine diphosphate (ADP)-ribosylation factor-like GTPase 4D (ARL4D) and tribbles pseudokinase 3 (TRIB3). When comparing SIRT7sh

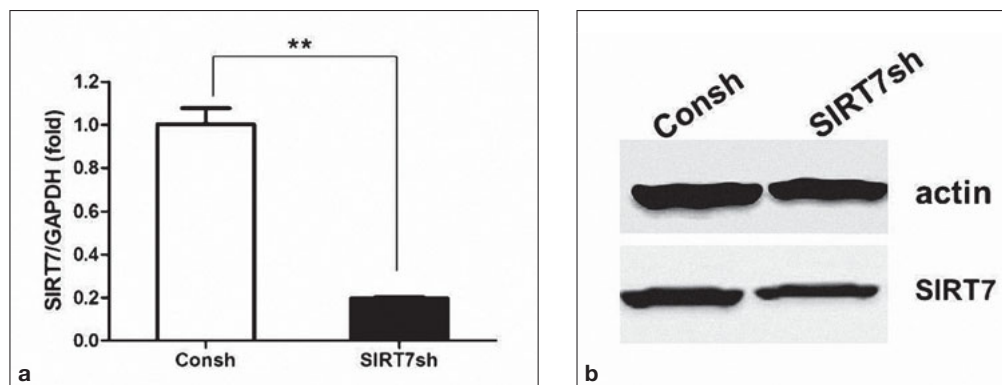


Fig 1 Identification of SIRT7 depletion in SCAP. SCAP were infected with shRNAs, which silenced SIRT7. **(a)** Real-time RT-PCR showed 80% depletion of SIRT7 expression. Actin was used as an internal reference gene. **(b)** Western blot results showed that SIRT7-shRNA effectively silenced SIRT7 expression.

SCAPs with Consh SCAPs, there were 553 upregulated lncRNA and 526 downregulated lncRNA. The top 10 evidently changed lncRNA are listed in Tables 3 and 4.

GO analysis of gene expression in SIRT7sh SCAPs compared to Consh SCAPs

To explore the function and possible mechanism of SIRT7 in SCAPs, RNA-seq was used to compare the changes in functional gene expression in these two

groups. The differentially expressed genes were subjected to GO analysis. According to the threshold, GO terms that were significantly regulated in the two groups with *P* value and FDR < 0.05 were identified. The value of -LgP (negative logarithm of the *P* value) represented the correlation between gene expression and the relevant biological process. As shown in Fig 2, the top significantly changed GO terms across SIRT7sh and Consh SCAPs were response to nucleus, cytoplasm, mitochondrion, protein binding, intrinsic apoptotic signal-

Table 1 Top 10 downregulated genes between SIRT7sh and Consh SCAPs.

Gene symbol	P value	Fold change	Gene feature
YWHAG	0.001	0.005	DOWN
VOPP1	0.024	0.016	DOWN
HSPB6	0.011	0.022	DOWN
DDIT4	0.011	0.041	DOWN
TNFAIP1	0.008	0.122	DOWN
PKIG	0.015	0.154	DOWN
YWHAQ	0.026	0.181	DOWN
CISD2	0.028	0.211	DOWN
CDK2AP1	0.003	0.266	DOWN
TOLLIP	0.047	0.234	DOWN

Table 3 Top 10 downregulated lncRNA between SIRT7sh and Consh SCAPs.

LncRNA_id	P value	Fold change	Target genes
ENST00000590168	0.015	0.010	RHBDF2
ENST00000509648	0.017	0.025	ANXA5
ENST00000588472	0.028	0.045	SDF2
ENST00000486898	0.019	0.049	MPV17
ENST00000526688	0.031	0.068	FGFR1
ENST00000506310	0.036	0.078	LMAN2
ENST00000494261	0.042	0.079	CLASP2
ENST00000491780	0.047	0.103	ARPC2
ENST00000481331	0.011	0.104	ATXN2
ENST00000593013	0.001	0.107	HDAC5

Table 2 Top 10 upregulated genes between SIRT7sh and Consh SCAPs.

Gene symbol	P value	Fold change	Gene feature
ARL4D	0.037	48.839	UP
TAF9	0.035	25.919	UP
MT-TS1	0.016	17.950	UP
TRIB3	0.017	12.089	UP
JDP2	0.040	9.338	UP
RPS15	0.001	7.425	UP
WASF2	0.018	6.362	UP
CDC42EP1	0.012	5.560	UP
CHMP3	0.002	5.500	UP
MYDGF	0.006	5.356	UP

Table 4 Top 10 upregulated lncRNA between SIRT7sh and Consh SCAPs.

LncRNA_id	P value	Fold change	Target genes
ENST00000597607	0.024	129.45	TECR
ENST00000556587	0.042	83.65	SRSF5
ENST00000475895	0.043	41.09	MRPS5
ENST00000602167	0.032	28.43	MAP2K2
ENST00000593146	0.007	25.79	APC2
ENST00000514306	0.042	25.32	PLK2
ENST00000571210	0.014	22.24	MFAP4
ENST00000314351	0.016	22.19	ADAMTS6
ENST00000494026	0.014	16.89	MTA1
ENST00000542286	0.001	11.58	DDX55

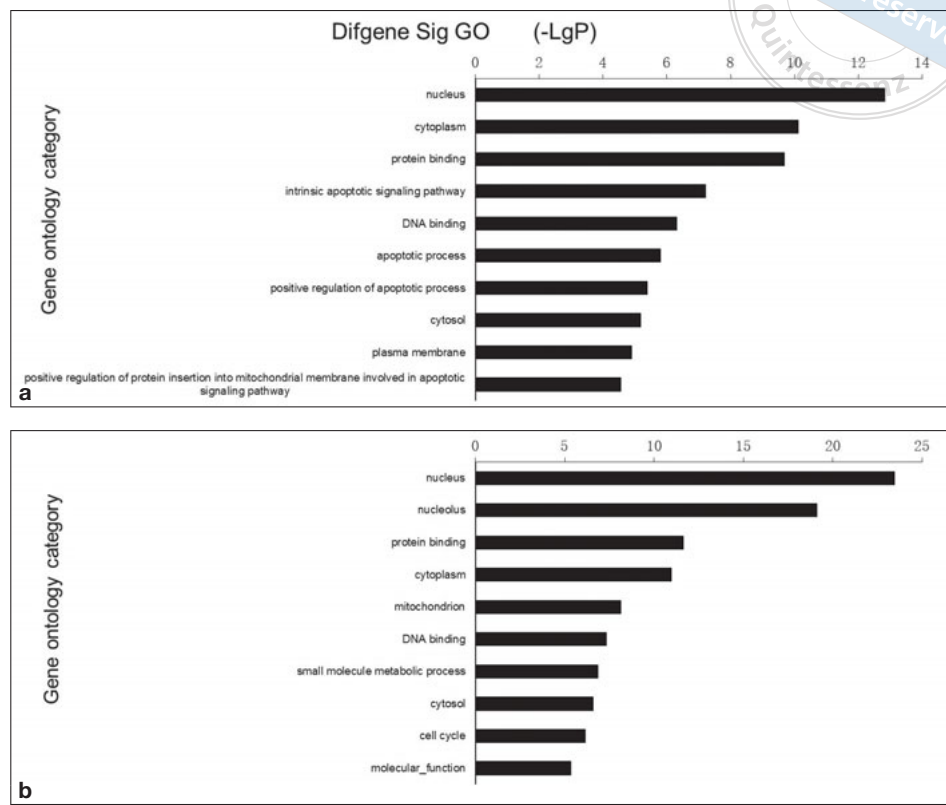


Fig 2 Significantly changed GO terms of differentially expressed genes. **(a)** The top 10 downregulated GOs targeted by SIRT7sh SCAPs compared to control SCAPs. **(b)** The top 10 upregulated GOs targeted by SIRT7sh SCAPs compared to control SCAPs. The y-axis shows GO category and the x-axis shows the $-LgP$. A larger $-LgP$ indicates a smaller P value.

ling pathway, DNA binding, apoptotic process, positive regulation of apoptotic process, cytosol, plasma membrane, small molecule metabolic process, cell cycle and molecular function. GO analysis clearly showed that many important functions, such as positive regulation of apoptotic process, cell cycle and small molecule metabolic process, were significantly different between the two groups, which were involved in cells' self-renewal ability and metabolic process.

Analysis of pathways in SIRT7sh SCAPs compared to Consh SCAPs

Based on the KEGG database, we analysed the top 10 pathways in both groups. As shown in Fig 3, some important pathways including metabolic, PI3K/Akt signalling, p53 signalling, viral carcinogenesis, apoptosis, proteoglycans in cancer, toll-like receptor signalling, amyotrophic lateral sclerosis (ALS), pyrimidine metabolism, ErbB signalling, Vibrio cholerae infection, biosynthesis of amino acids, cell cycle, insulin signalling, ribosome biogenesis in eukaryotes, basal transcription factors and non-homologous end-joining were significantly different between the two groups.

GSEA in SIRT7sh SCAPs compared to Consh SCAPs

To investigate the potential altered pathways in the two groups, GSEA was implemented between SIRT7sh SCAPs and Consh SCAPs. Based on the result of GSEA, genes were mainly enriched in cell cycle process (Fig 4a) and cell proliferation (Fig 4b). Moreover, we noticed that the TGF- β signalling and cytokine-cytokine receptor interaction pathways were also significantly enriched (Figs 4c and 4d).

Discussion

In the present study, we performed RNA-seq analysis between SIRT7sh SCAPs and Consh SCAPs to explore the possible function and mechanism of SIRT7 on SCAPs. In our study, GO analysis revealed particular enriched functional pathways among the genes responsible for the divergent features of the two groups. These data demonstrated that SIRT7 may play an important role in the survival, self-renewal and apoptosis of SCAPs because metabolic, apoptosis and cell cycle pathways are involved. Furthermore, we identified that the PI3K/Akt signalling, p53 signalling, viral carcinogenesis, toll-

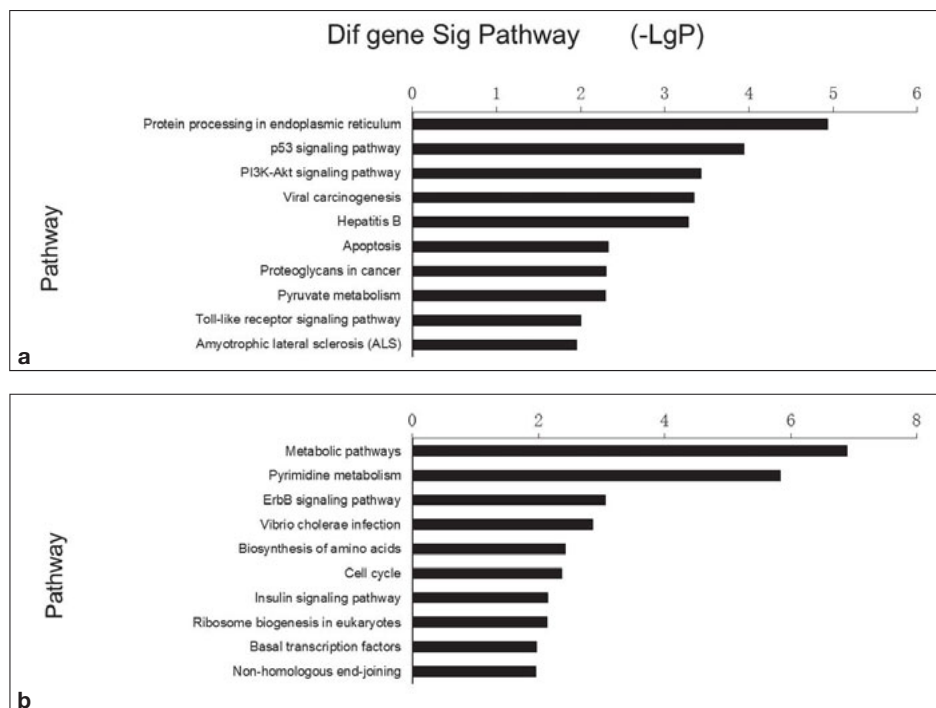


Fig 3 Significantly changed pathways. Based on the KEGG database, pathways with $P < 0.05$ and $FDR < 0.05$ were identified as significantly changed. **(a)** Significantly downregulated pathways targeted by SIRT7sh SCAP compared to control SCAP. **(b)** Significantly upregulated pathways targeted by SIRT7sh SCAP compared to control SCAP. The y-axis shows significantly changed pathways and the x-axis shows the $-LgP$. A larger $-LgP$ indicates a smaller P value.

like receptor signalling and insulin signalling pathways may be involved in the function of SIRT7 in SCAPs.

SIRT7 is the least understood member of the human sirtuin family and influences multiple biological processes. Initially, SIRT7 was reported to be positively correlated with cell proliferation. In metabolically active cells, SIRT7 was highly expressed, whereas its expression was very low in non-proliferating cells^{22,23}. However, in a murine model and cell lines, SIRT7 was demonstrated to play an antiproliferative role and to be inversely correlated with tumourigenic potential²⁴. In the present study, silencing of SIRT7 in SCAPs led to significant changes in genes involved in cell proliferation and apoptosis, which indicates that SIRT7 may affect the proliferation function of SCAPs. In SIRT7sh SCAPs, YWHAG was downregulated 200-fold compared to its expression in Consh SCAPs. YWHAG is one of the 14-3-3 family isoforms, and functions as a scaffold in multiprotein complexes and is thus involved in several cellular processes as regulatory molecules including cell survival, apoptosis, protein trafficking and cell cycle regulation²⁵⁻²⁷. Further study is therefore needed to determine whether YWHAG could be considered a potential target gene of SIRT7, which regulates the survival of SCAPs. The present results also showed that SIRT7 could directly affect cell cycle-related genes and the G2/M checkpoint, which further illustrates the role played by SIRT7 in the proliferation of SCAPs.

Some recent studies have established the emerging role played by SIRT7 in age-related processes. On one hand, SIRT7 has been found to be directly related to senescence, illustrated by the fact that SIRT7 knockout mice had a shorter lifespan and SIRT7 expression was reduced in aged HSCs^{9,28}. On the other hand, over-expression of SIRT7 delayed stress-induced premature senescence when responding to external stress signals²⁹. SIRT7 was also reported to be regulated by miR-152 in DPSC senescence¹⁰. In the present study, SIRT7 silencing greatly decreased the expression of CSD2 and CDK2AP1, both of which play important roles in senescence. CSD2, an evolutionarily conserved novel gene, encodes a transmembrane protein primarily associated with the mitochondrial outer membrane. CSD2 deficiency in mice caused mitochondrial breakdown and premature ageing^{30,31}. However, in CSD2 transgenic mice, a persistent level of CSD2 expression gave the mice a long-lived phenotype that was linked to extending healthy lifespan and delaying age-related diseases³². It was therefore speculated that SIRT7 may influence SCAP senescence through the regulation of CSD2 expression. CDK2AP1 also showed a correlation with stem cell differentiation and self-renewal. Knockdown of CDK2AP1 in cells resulted in a significant reduction in the expression of pluripotency genes, increased expression of p53 and enhanced differentiation capacity, which may cause premature senescence³³⁻³⁵.

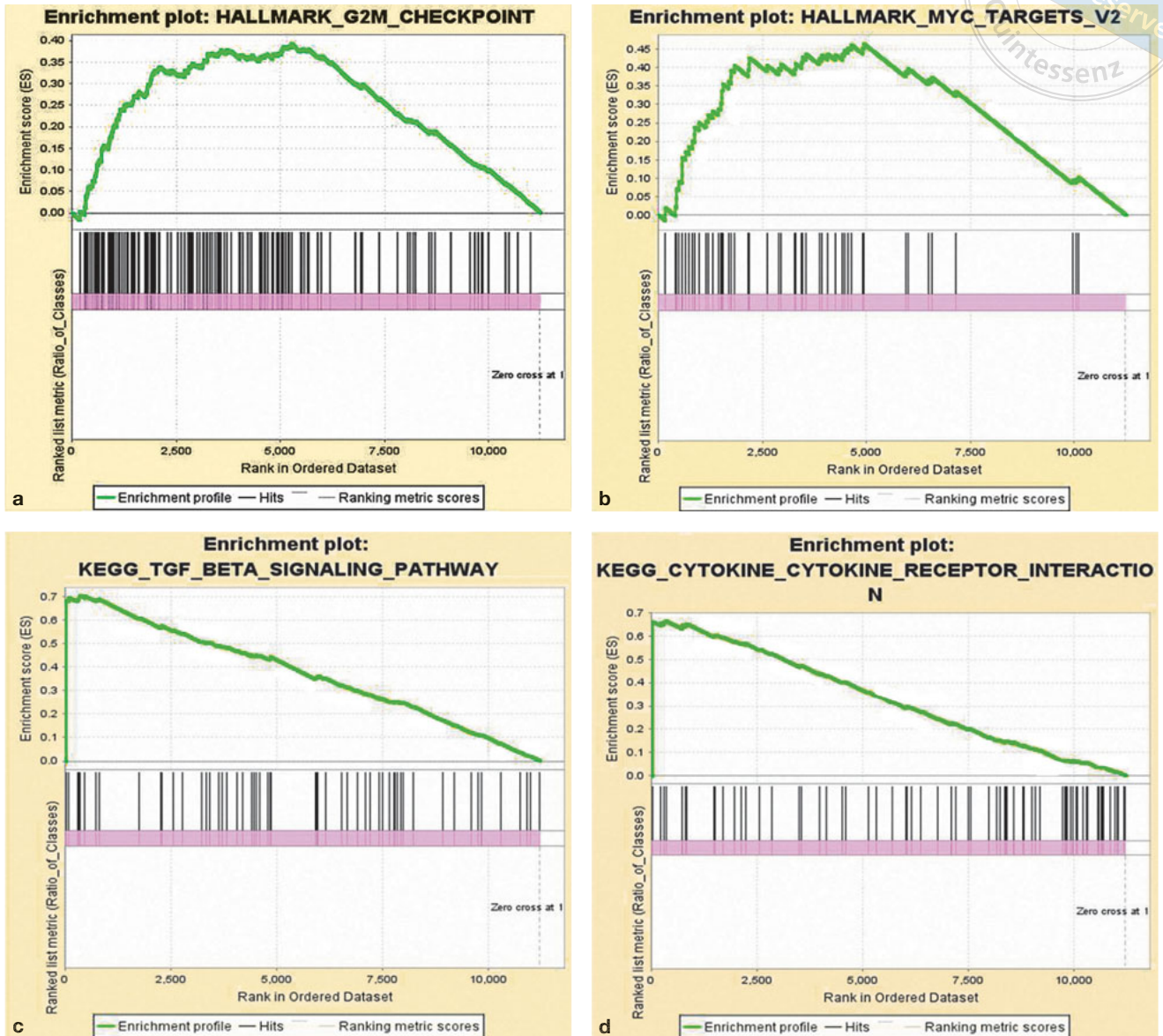


Fig 4 GSEA of the co-expressed genes. **(a)** G2/M GSEA. **(b)** MYC GSEA. **(c)** TGF- β pathway GSEA. **(d)** Cytokine–cytokine receptor interaction GSEA.

Conclusion

Based on these results, it is speculated that SIRT7 may play an important role in SCAP senescence. In addition, the effect of SIRT7 on cell differentiation was also addressed. SIRT7 activation can improve the regenerative capacity of aged HSCs³⁶. SIRT7 also negatively regulated the osteogenic capacity of hBMSCs¹¹. SIRT7 knockout mice, meanwhile, developed severe osteopenia, and SIRT7 positively enhanced the osteogenic potential of mouse osteoblasts³⁷. In the present study, genes related to

cell differentiation, such as TRIB3 and CDK2AP1^{33,38}, were involved, indicating that SIRT7 may play a role in regulating the differentiation of SCAPs.

This study provides some indications of the impact of SIRT7 on SCAPs; however, further study is needed to explore its specific function and mechanism in SCAPs.

Conflicts of interest

The authors declare no conflicts of interest related to this study.

Author contribution

Dr Lu Yuan JIN performed the experiment, participated in the data analysis and interpretation and drafted the manuscript; Drs Lei HU and Hui Na LIU participated in the collection and/or assembly of the data; Dr Deng Sheng XIA was responsible for the study conception and design and helped to draft the manuscript; Dr Zhi Peng FAN was responsible for the study conception and design, data analysis and interpretation, manuscript writing and final revision. All the authors read and approved the final manuscript.

(Received Apr 17, 2019; accepted Feb 17, 2020)

References

1. Sonoyama W, Liu Y, Yamaza T, et al. Characterization of the apical papilla and its residing stem cells from human immature permanent teeth: a pilot study. *J Endod* 2008;34:166–171.
2. Patil R, Kumar BM, Lee WJ, et al. Multilineage potential and proteomic profiling of human dental stem cells derived from a single donor. *Exp Cell Res* 2014;320:92–107.
3. Kang J, Fan W, Deng Q, He H, Huang F. Stem cells from the apical papilla: a promising source for stem cell-based therapy. *Biomed Res Int* 2019;2019:6104738.
4. O'Callaghan C, Vassilopoulos A. Sirtuins at the crossroads of stemness, aging, and cancer. *Aging Cell* 2017;16:1208–1218.
5. Preyat N, Leo O. Sirtuin deacylases: a molecular link between metabolism and immunity. *J Leukoc Biol* 2013;93:669–680.
6. Liu T, Liu PY, Marshall GM. The critical role of the class III histone deacetylase SIRT1 in cancer. *Cancer Res* 2009;69:1702–1705.
7. Kanfi Y, Naiman S, Amir G, et al. The sirtuin SIRT6 regulates lifespan in male mice. *Nature* 2012;483:218–221.
8. Houtkooper RH, Pirinen E, Auwerx J. Sirtuins as regulators of metabolism and healthspan. *Nat Rev Mol Cell Biol* 2012;13:225–238.
9. Mohrin M, Shin J, Liu Y, et al. Stem cell aging. A mitochondrial UPR-mediated metabolic checkpoint regulates hematopoietic stem cell aging. *Science* 2015;347:1374–1377.
10. Gu S, Ran S, Liu B, Liang J. miR-152 induces human dental pulp stem cell senescence by inhibiting SIRT7 expression. *FEBS Lett* 2016;590:1123–1131.
11. Chen EEM, Zhang W, Ye CCY, et al. Knockdown of SIRT7 enhances the osteogenic differentiation of human bone marrow mesenchymal stem cells partly via activation of the Wnt/ β -catenin signaling pathway. *Cell Death Dis* 2017;8:e3042.
12. Jang YE, Go SH, Lee BN, et al. Changes in SIRT gene expression during odontoblastic differentiation of human dental pulp cells. *Restor Dent Endod* 2015;40:223–228.
13. Trapnell C, Pachter L, Salzberg SL. TopHat: discovering splice junctions with RNA-seq. *Bioinformatics* 2009;25:1105–1111.
14. Trapnell C, Williams BA, Pertea G, et al. Transcript assembly and quantification by RNA-seq reveals unannotated transcripts and isoform switching during cell differentiation. *Nat Biotechnol* 2010;28:511–515.
15. Yu G, Wang LG, Han Y, He QY. clusterProfiler: an R package for comparing biological themes among gene clusters. *OMICS* 2012;16:284–287.
16. Hirsch T, Rothoef T, Teig N, et al. Regeneration of the entire human epidermis using transgenic stem cells. *Nature* 2017;551:327–332.
17. Kong L, Zhang Y, Ye ZQ, et al. CPC: assess the protein-coding potential of transcripts using sequence features and support vector machine. *Nucleic Acids Res* 2007;35:W345–W349.
18. Sun L, Luo H, Bu D, et al. Utilizing sequence intrinsic composition to classify protein-coding and long non-coding transcripts. *Nucleic Acids Res* 2013;41:e166.
19. Sun L, Zhang Z, Bailey TL, et al. Prediction of novel long non-coding RNAs based on RNA-seq data of mouse Klf1 knockout study. *BMC Bioinformatics* 2012;13:331.
20. Tafer H, Hofacker IL. RNAplex: a fast tool for RNA-RNA interaction search. *Bioinformatics* 2008;24:2657–2663.
21. Tao T, Yang X, Zheng J, et al. PDZK1 inhibits the development and progression of renal cell carcinoma by suppression of SHP-1 phosphorylation. *Oncogene* 2017;36:6119–6131.
22. Michishita E, Park JY, Burneskis JM, Barrett JC, Horikawa I. Evolutionarily conserved and nonconserved cellular localizations and functions of human SIRT proteins. *Mol Biol Cell* 2005;16:4623–4635.
23. Ford E, Voit R, Liszt G, Magin C, Grummt I, Guarente L. Mammalian Sir2 homolog SIRT7 is an activator of RNA polymerase I transcription. *Genes Dev* 2006;20:1075–1080.
24. Vakhrusheva O, Braeuer D, Liu Z, Braun T, Bober E. Sirt7-dependent inhibition of cell growth and proliferation might be instrumental to mediate tissue integrity during aging. *J Physiol Pharmacol* 2008;59(Suppl 9):201–212.
25. Du C, Zhang C, Hassan S, Biswas MH, Balaji KC. Protein kinase D1 suppresses epithelial-to-mesenchymal transition through phosphorylation of snail. *Cancer Res* 2010;70:7810–7819.
26. Hou Z, Peng H, White DE, et al. 14-3-3 binding sites in the snail protein are essential for snail-mediated transcriptional repression and epithelial-mesenchymal differentiation. *Cancer Res* 2010;70:4385–4393.
27. Freeman AK, Morrison DK. 14-3-3 Proteins: diverse functions in cell proliferation and cancer progression. *Semin Cell Dev Biol* 2011;22:681–687.
28. Vakhrusheva O, Smolka C, Gajawada P, et al. Sirt7 increases stress resistance of cardiomyocytes and prevents apoptosis and inflammatory cardiomyopathy in mice. *Circ Res* 2008;102:703–710.
29. Kiran S, Chatterjee N, Singh S, Kaul SC, Wadhwa R, Ramakrishna G. Intracellular distribution of human SIRT7 and mapping of the nuclear/nucleolar localization signal. *FEBS J* 2013;280:3451–3466.
30. Chen YF, Kao CH, Kirby R, Tsai TF. Cisd2 mediates mitochondrial integrity and life span in mammals. *Autophagy* 2009;5:1043–1045.
31. Chen YF, Kao CH, Chen YT, et al. Cisd2 deficiency drives premature aging and causes mitochondria-mediated defects in mice. *Genes Dev* 2009;23:1183–1194.
32. Wang CH, Kao CH, Chen YF, Wei YH, Tsai TF. Cisd2 mediates lifespan: is there an interconnection among Ca²⁺ homeostasis, autophagy, and lifespan? *Free Radic Res* 2014;48:1109–1114.
33. Alsayegh KN, Sheridan SD, Iyer S, Rao RR. Knockdown of CDK2AP1 in human embryonic stem cells reduces the threshold of differentiation. *PLoS One* 2018;13:e0196817.
34. Wong DT, Kim JJ, Khalid O, Sun HH, Kim Y. Double edge: CDK2AP1 in cell-cycle regulation and epigenetic regulation. *J Dent Res* 2012;91:235–241.
35. Alsayegh KN, Gadepalli VS, Iyer S, Rao RR. Knockdown of CDK2AP1 in primary human fibroblasts induces p53 dependent senescence. *PLoS One* 2015;10:e0120782.
36. Haynes CM, Fiorese CJ, Lin YF. Evaluating and responding to mitochondrial dysfunction: the mitochondrial unfolded-protein response and beyond. *Trends Cell Biol* 2013;23:311–318.
37. Fukuda M, Yoshizawa T, Karim MF, et al. SIRT7 has a critical role in bone formation by regulating lysine acylation of SP7/Osterix. *Nat Commun* 2018;9:2833.
38. Zhang C, Hong FF, Wang CC, et al. TRIB3 inhibits proliferation and promotes osteogenesis in hBMSCs by regulating the ERK1/2 signaling pathway. *Sci Rep* 2017;7:10342.